J Mater Sci: Mater Electron (2015) 26:2248–2256
DOI 10.1007/s10854-015-2677-0

Engineering *V*O, C_iO_i and C_iC_s defects in irradiated Si through Ge and Pb doping

C. A. Londos · T. Angeletos · E. N. Sgourou · A. Chroneos

Received: 12 November 2014 / Accepted: 5 January 2015 / Published online: 21 January 2015

Abstract Carbon and oxygen associated defects such as *V*O, C_iO_i and C_iC_s are common in electron irradiated silicon. Their presence can affect the material and electronic properties of Si. A way to limit their impact and understand their behavior is through doping with large isovalent dopants. The aim of the present study is to investigate and compare the effect of Ge and Pb doping on *V*O, C_iO_i and C_iC_s defects in electron irradiated Si mainly by using Fourier transform infrared spectroscopy in conjunction with recent density functional theory calculations. It was determined that the production of these defects is reduced by the presence of the isovalent impurity and more significantly for Pb doping as compared to Ge doping. Upon annealing the conversion to secondary defects (in particular *V*O to VO_2 and C_iO_i to C_sO_{2i}) is also affected by the isovalent dopants. Interestingly, the conversion ratio a_{VO2}/a_{VO} is reduced with the increase of the isovalent radius, whereas the a_{CsO2i}/a_{CiOi} is enhanced. Theoretical calculations were used to corroborate these findings.

C. A. Londos · T. Angeletos · E. N. Sgourou
Solid State Physics Section, University of Athens, Panepistimiopolis Zografos, 157 84 Athens, Greece
e-mail: hlontos@phys.uoa.gr

A. Chroneos (✉)
Department of Materials, Imperial College London, London SW7 2AZ, UK
e-mail: alexander.chroneos@imperial.ac.uk

A. Chroneos
Faculty of Engineering and Computing, Coventry University, Priory Street, Coventry CV1 5FB, UK

1 Introduction

Si remains the principal material for a wide range of nanoelectronic, sensor and photovoltaic devices [1–5]. Defects processes are very important as the characteristic dimensions of devices are a few nanometers. The detailed understanding of many defect processes that can affect material and devices properties is not well established [6–10]. Carbon (C) and oxygen (O) impurities are the most common and important impurities in electron irradiated Si.

FTIR has been used extensively to study the production and annealing behavior of defects in irradiated Si. Localised Vibrational Modes (LVM) bands arising from oxygen-related and carbon-related defects in Si have been correlated and attributed to particular defects. The band at 830 cm^{-1} has been assigned [11, 12] to the neutral charge state of the *V*O defect (A-center), which is the archetypal oxygen-related defect in Si. The C_iO_i and the C_iC_s defects are very important carbon-related defects. At least six LVM bands have been assigned [13] to the C_iO_i center (strongest is at $\sim$865 cm^{-1}). The C_iC_s defect is metastable, with five IR bands been correlated with the A configuration of the defect and another six IR bands with the B configuration of the defect. Although the bands are very weak and can be seen only at liquid He temperatures [14], a band at 544 cm^{-1} can also be detected [15] at room temperature in carbon-rich Si. In essense the latter band appears to be the superposition of two bands [15, 16] one related with the C_iC_s defect and the other with the C_iO_i defect. Regarding the C_iC_s defect, a third configuration has been identified [17, 18] recently renewing the interest [19] in the study of carbon-related defects.

Importantly, the *V*O, the C_iO_i and the C_iC_s defects introduce electrical levels [3, 13, 20–22] in the forbidden gap of Si affecting the quality and the efficiency of Si-

based devices. This enhances the need to investigate the properties of these defects with the aim to suppress their negative impact on the output of devices and to control their behavior. Isovalent doping is one of the techniques used to this end.

From a theoretical perspective recent studies employing density functional theory (DFT) have been used to investigate the structure and properties of oxygen and carbon related defects in Si [23–25]. DFT is a valuable tool to investigate the electronic structure and defect processes of defects in Si. For example, studies on oversized dopant atoms (Sn or Pb) in Si are in excellent agreement with experiment in the suppresion of the formation of *V*O defects [24].

In this study (among the isovalent dopants Ge, Sn and Pb) we decided to investigate and compare the effect of Ge and Pb doping in RT irradiated Cz-Si containing equal concentrations of carbon. Notably, both Ge and Pb do not introduce energy levels related to radiation-induced defects in the forbidden gap of Si in contrast to Sn. Regarding vacancies, Sn produces Sn*V* pairs, which survive up to 150 °C. However, Ge produces Ge*V* pairs which do not survive RT and Pb in all indications produces Pb*V* pairs, although any signal from this defect has not been detected so far. On the other hand, in the case of carbon contained Sn-doped Cz-Si, SnC related defects are produced which introduce levels in the gap that have a negative effect in the radiation tolerance of Si material. In the case of Ge doping any GeC related defects have not been reported and in the case of Pb doping although there are indications for the existence of PbC related defects any definite assignment has not been made so far. Importantly, in Pb-doped Si carbon is usually introduced as a co-dopant. Carbon has a smaller (than Si) covalent radius and it is introduced in order to relieve strains in the lattice induced by Pb due to its larger (than Si) covalent radius. Also carbon retains Pb at substitutional sites avoiding the formation of Pb precipitates. Thus for comparison purposes we also use in this study C-containing Ge-doped Si, with carbon in approximately the same concentration as in Pb-doped Si, in order to compare the exact difference between Pb and Ge doping. Remarkably, a radiation-induced level in Cz-Si at E_c −0.37 eV is avoided [26] in Pb-doped Si. This is an additional benefit of Pb doping that one has to consider in manufacturing a radiation hard material. It is also known [27] that Pb increases the carrier's lifetime in Si. As a result the optoelectronic properties of Si are improving, leading to an enhancement of the performance of polycrystalline Si for applications in solar cells. Ge-doped Si is also used in photovoltaic industry to enhance the conversion efficiency of solar cells [28, 29]. Thus it is of technological interest to gather all the relevant information about the impact of the two dopants on the behaviour of radiation defects.

In the present study we compare the impact of the isovalent impurities Ge and Pb on the production and conversion to secondary defects of *V*O, C_iO_i and C_iC_s defects in electron irradiated Si. Additionally, we calculate the induced strains and discuss their impact on the defect energetics. The results are discussed in view of recent computational and theoretical findings.

2 Methodology

We used three samples cut from prepolished Czochralski Si (Cz-Si) wafers. One group of Cz-Si samples contained carbon (labeled CCz-Si), another one contained Ge and C (labeled CCz-Si:Ge) and another one contained Pb and C (labeled CCz-Si:Pb). The Ge and Pb concentrations of the samples were determined using secondary ion mass spectrometry (SIMS) and their values were given by the provider of the samples. The carbon (606 cm^{-1}) and oxygen (1,106 cm^{-1}) concentrations were calculated by infrared spectroscopy using calibration coefficients 1.0×10^{17} cm^{-2} and 3.14×10^{17} cm^{-2}, respectively. The carbon concentration of all the samples was of the same order. The C, O, Ge and Pb concentrations are given in Table 1. The samples were irradiated with 2 MeV electrons with a fluence of 1×10^{18} cm^{-2} at about 80 °C, using the Dynamitron accelerator at Takasaki-JAERI (Japan). After the irradiation, all the samples were subjected to isochronal anneals up to 600 °C in open furnaces in steps of 10 °C and 20 min duration. After each annealing step, the IR spectra were recorded at room temperature by means of a Fourier Transform Infrared spectrometer (JASCO-470 plus) with a resolution of 1 cm^{-1}. The two phonon background absorption was subtracted from each spectrum by using a float-zone sample of equal thickness.

3 Results

Figure 1a–c represent characteristic segments of the infrared spectra of the CCz-Si, CCz-Si:Ge and CCz-Si:Pb samples, respectively, recorded after irradiation and at the temperature of 350 °C in the course of the 20 min isochronal anneals sequence. Bands at 830 cm^{-1} (*V*O), at 861 cm^{-1} (C_iO_i), at 546 cm^{-1} (C_iC_s/C_iO_i), and pair of bands at (936, 1,020) cm^{-1} ($C_iO_i(Si)_I$) are present in all the samples, as expected. Importantly, a band at ~1,020 cm^{-1} appearing in the spectra at 350 °C is different than the band at 1,020 cm^{-1} appearing in the spectra immediately after irradiation and which together with the 936 cm^{-1} band constitute a pair attributed to the $C_iO_i(Si)_I$ defect, which is stable [30] up to around 180 °C. The 1,020 cm^{-1} band shown at 350 °C in the spectra seems to emerge in the

Table 1 The initial oxygen, carbon and isovalent impurity content of the samples used

Sample name	Isovalent impurity			$[O_i]_o$ 10^{17} cm^{-3}	$[C_s]_o$ 10^{17} cm^{-3}
	Element	Radius (A)	Content (cm^{-3})		
CCz-Si	C	0.77	1.6×10^{17}	10.00	1.6
CCz-Si:Ge	Ge	1.22	4×10^{18}	5.55	1.0
CCz-Si:Pb	Pb	1.46	1×10^{18}	2.1	0.95

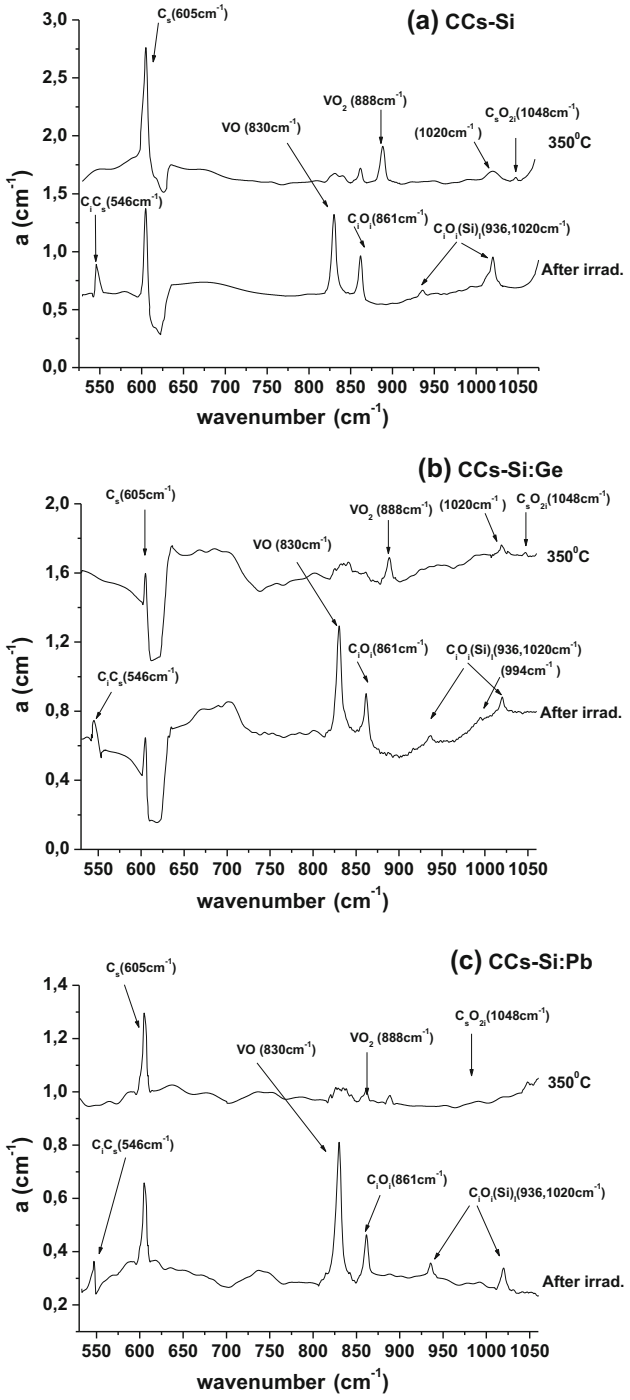

Fig. 1 Segments of the infrared spectra of the samples for **a** CCz-Si, **b** CCz-Si:Ge and **c** CCz-Si:Pb after irradiation and at 350 °C

spectra upon the disappearance of the 546 cm^{-1} band. This indicates a possible correlation with this defect in the sense that is produced upon the annealing out of the structures C_iO_i/C_iC_s related with the 546 cm^{-1} band. The corresponding signal is very weak to allow proper analysis with Lorentzian profiling in order to have the exact contribution of each of the C_iO_i and C_iC_s structures in the shape of the 546 cm^{-1} band. The origin of the 1,020 cm^{-1} band is not known. However, since the C_iO_i upon annealing mostly dissociates, although a small part contributes in the formation of the 1,048 cm^{-1} band attributed [31] to the C_sO_{2i} defect, one may correlate the 1,020 cm^{-1} band with annealing processes related with the C_iC_s defect. In this sense, in Fig. 2 the 546 and the 1,020 cm^{-1} bands are considered together.

Figure 2a–c represent the thermal evolution of (*V*O, VO_2), (C_iO_i, C_sO_{2i}) and (C_iC_s/C_iO_i, 1,020 cm^{-1}) defects of the CCz-Si(a), CCz-Si:Ge(b) and CCz-Si:Pb(c), respectively. Notably, for the CCz-Si:Pb sample the 1,020 cm^{-1} band is very weak and its evolution cannot be shown in the Fig. 2c. Furthermore, the VO_2 band is largerly suppressed in the latter sample. Interestingly, the suppression of the VO_2 band due to Pb doping (with [Pb] = 10^{18} cm^{-1}) is almost the same with the suppression of VO_2 in *n*-type and *p*-type $Si_{1-x}Ge_x$ material [32, 33] with x = 5.6 % that is with Ge content at least three orders of magnitude larger than that of Pb.

Figure 3 shows the production of the *V*O, C_iO_i and C_iC_s/C_iO_i versus covalent radius of the isovalent dopant. Clearly, a_{VO} decreases when the magnitude of the dopant increases.

Figure 4 shows the conversion ratios a_{VO2}/a_{VO} and a_{CsO2i}/a_{CiOi} versus covalent radius of the isovalent dopant. Clearly the two ratios exhibit a dependence to the covalent radius of the dopant. It is observed that ratio a_{VO2}/a_{VO} decreases with the increase of the covalent radius of the dopant, whereas the ratio a_{CsO2i}/a_{CiOi} shows the opposite trend.

4 Discussion

4.1 Background

The principal aim of the present contribution is to discuss the FTIR results, review recent DFT calculations and

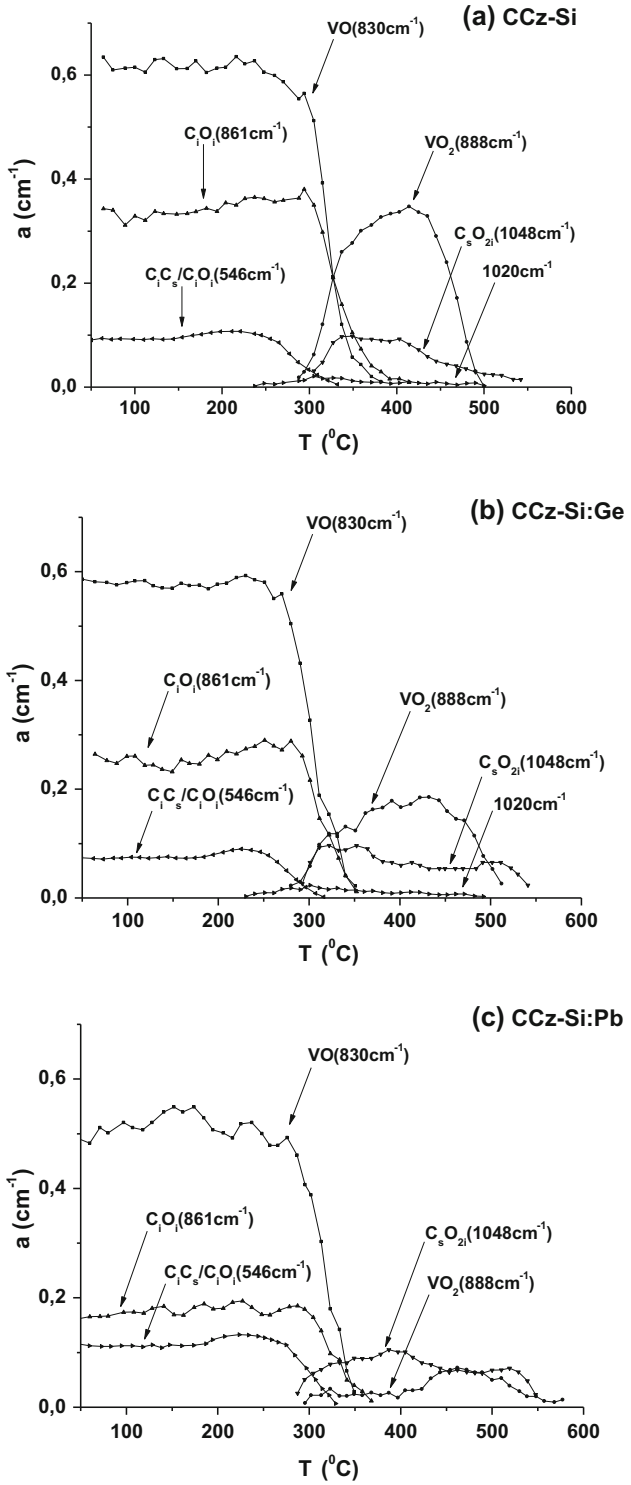

Fig. 2 The evolutions of the (*V*O, *V*O$_2$), (C_iO_i, C_sO_{2i}) and (C_iC_s/C_iO_i, 1,020 cm^{-1}) defects upon annealing up to 600 °C

deconvolute the physical reasons why Pb doping is different to Ge doping in the production and formation of defects in Si. In particular we examine the impact of Pb and Ge doping on the production of *V*O, C_iO_i and C_iC_s in

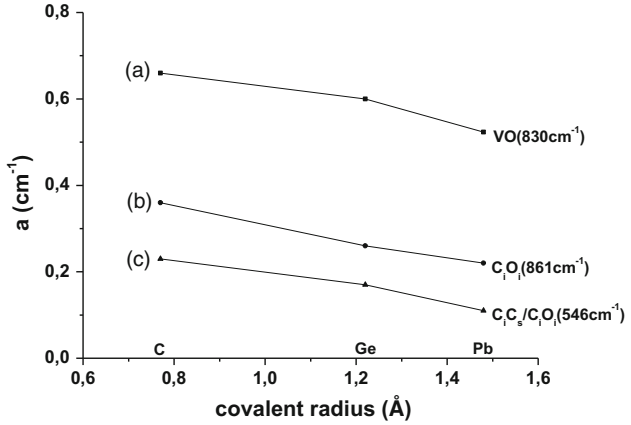

Fig. 3 The production (absorption coefficient) of the *V*O, C_iO_i and C_iC_s/C_iO_i defects as a function of the isovalent dopant radius

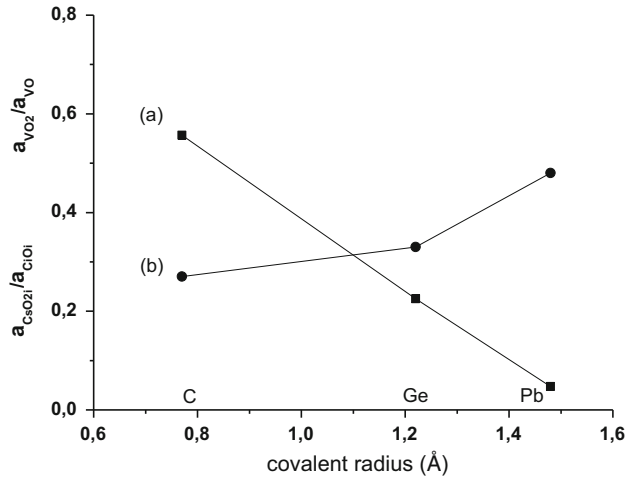

Fig. 4 The conversion ratio (a_{VO2}/a_{VO}) and (a_{CsO2i}/a_{CiOi}) as a function of the isovalent dopant radius

electron irradiated Si and their subsequent conversion to secondary defects. To consider the differences between the two dopants one needs to examine (a) the dopant strain energies, (b) the strain in the lattice due to isovalent doping and (c) the energetics of their association with the constituent elements of the *V*O, C_iO_i and C_iC_s defects namely the *V*, O_i, C_i and C_s and in that respect recent DFT studies are reviewed.

4.2 Dopant strain energies in Si

Ge and Pb substitutional atoms induce compressive elastic strains in the Si lattice. This is due to their larger tetrahedral covalent radii, compared to that of the Si atom. Let the Δr represent the difference of the tetrahedral radius between the Si atom and the dopant. Due to the presence of the larger dopant the first and the second nearest neighbors (NNs) move radially outwards [34] by an amount of Δr_1

and Δr_2 respectively and so on for the higher order NNs. It is reasonable that $\Delta r > \Delta r_1 > \Delta r_2 > \ldots$ as a result of the compression of the dopant-Si bonds. Neglecting the atomistic nature of the displacements beyond the first NNs and considering the Si lattice as a continuous medium, we can apply the Hooke's law to estimate the strain energy stored in the first NN of the dopant atoms. This can be expressed as follows:

$$E^{st} = 4 \times \frac{1}{2} g K_c (\Delta r - \Delta r_1)^2 + 8\pi G r_0 (\Delta r_1)^2 \quad (1)$$

where gK_c represents the stiffness constant of the impurity-1st NNs bonds (Kc is the force constant and g is a dimensionless parameter of order unity) and the last term of equation represents the energy stored in the surrounding lattice matrix by the expansion of a cavity of radius r_0 by an amount Δr_1. Here, r_0 is the interatomic distance in the Si lattice and G is the Si shear modulus of elasticity. Formula (1) can be written as follows [34]:

$$E^{st} = const \times (\Delta r)^2 \quad (2)$$

The increase of the tetrahedral radius in each case is calculated by the expression $\Delta r = r_d - r_{Si}$, where r_d is the covalent radius of the impurity atom and r_{Si} is this of a Si atom ($r_{si} = 1.17$ Å). Considering that the covalent radii of Ge and Pb are $r_{Ge} = 1.22$ Å and $r_{Pb} = 1.4$ Å respectively, we have $\Delta r_{Ge} = 0.05$ Å and $\Delta r_{Pb} = 0.05$ Å respectively. Comparing the strain energy stored in the first NNs of the Pb and Ge atoms:

$$\frac{E^{st}_{Pb}}{E^{st}_{Ge}} = \left(\frac{\Delta r_{Pb}}{\Delta r_{Ge}}\right)^2 \cong 1.39$$

This indicates that the strain energy in the case of Pb is greater than this of the Ge. So it is more preferable for the Pb defect to trap vacancies in order to decrease the strain energy, compared to Ge.

4.3 Strain in the Si lattice due to isovalent doping

The relative change of volume $\frac{\Delta V}{V_0}$ due to the presence of the dopant, is connected with the change υ^d of the volume V_o due to the replacement of one Si atom by the dopant atom [35]. The relative relation is given by $\frac{\Delta V}{V_0} = \frac{n}{N}\left(\frac{\upsilon^d}{\upsilon^{Si}}\right)$, where υ^{Si} is the volume that corresponds to the Si atom and V_0 stands for the volume of the pure Si crystal. Assuming that the atoms in the Si lattice behave like hard spheres, the relative volume change $\frac{\Delta V}{V_0}$ can be expressed as follows:

$$\frac{\Delta V}{V_0} = \frac{n}{N}\frac{\frac{4}{3}\pi\left(R_d^3 - R_{Si}^3\right)}{\frac{4}{3}\pi R_{Si}^3} = \frac{n}{N}\left[\left(\frac{R_d}{R_{Si}}\right)^3 - 1\right] \quad (3)$$

where n, R_d and N, R_{Si} are the concentration and the covalent radius of the dopant and the Si atom, respectively. From relation (3) the values $\frac{\Delta V}{V_0} = 1.07 \times 10^{-5}$ and $\frac{\Delta V}{V_0} = 1.73 \times 10^{-5}$ for the Ge and Pb dopants, respectively. To estimate the stress related to the presence of the larger impurity atoms in the Si lattice we consider that the induced pressure P produces a change in the unit cell volume. The relative change $\frac{\Delta V}{V_0}$ in the volume of the undoped Si crystal can be derived from the empirical formula [36]:

$$\frac{\Delta V}{V_0} = a_0 + aP + bP^2 + cP^3 + \cdots \quad (4)$$

where in the case of Si, the coefficients are $\alpha_0 = 0$, $\alpha = 10.211 \times 10^{-4}$ kbar^{-1}, $b = -2.9614 \times 10^{-6}$ kbar^{-2} and $c = 0$ kbar^{-3}. To simplify our calculations, we take into account only the first important term of the above sum αP, since the terms of the second order and higher are very small compared with the first. Thus, replacing the above calculated values of $\frac{\Delta V}{V_0}$ for the case of Ge and Pb in the final relation $\frac{\Delta V}{V_0} = \alpha P$ it is deduced that $P_{Ge} = 1.05 \times 10^{-2}$ kbar and $P_{Pb} = 1.69 \times 10^{-2}$ kbar, respectively. As we can see, the strain in the case of Pb is greater compared to that of the Ge, but in both cases the value is rather small to cause significant changes in the processes related with the production and annealing of the radiation defects.

4.4 Insights from DFT and other considerations

As it is found for the calculations above the dopant strain energies and the strain in the lattice due to isovalent doping are greater for Pb than Ge doping. The association of a V with an oversized isovalent atom such as Pb and Ge in Si is energetically favorable as the vacant space provided relaxes the strain associated with the accommodation of the oversized isovalent atom in the lattice. This is consistent with the calculated binding energies of the PbV and GeV which are −1.37 and −0.27 eV respectively (refer to Table 2). Note that the binding energy discussed in the present study refers to the energy difference between the defect cluster with respect to the energy of the system when the constituent defects are isolated. A negative binding energy implies that the defect cluster is energetically favourable over its component defects. The difference in the PbV and GeV pairs is not only quantitative (i.e. their 1.1 eV difference in binding energies) but also structural. In previous theoretical work Höhler et al. [23] calculated that the very big impurities in Si and Ge host lattices are accommodated in the split-vacancy configuration rather than the full-vacancy configuration. In the split vacancy configuration the dopant is surrounded by two semi-vacancies (i.e. it occupies the position in between two lattice sites), whereas in the full-vacancy configuration the

dopant is at a near substitutional site with a vacant nearest neighbor host atom site. Höhler et al. [23] did not consider Pb*V* defects, however, in recent DFT studies [24, 37] it was calculated that Pb*V* forms in the split-vacancy configuration whereas Ge*V* in the full-vacancy configuration.

Considering the experimental results and the insight from DFT calculations discussed above it can be concluded that the introduction of oversized isovalent atoms in the lattice leads to species competitive to O_i in the capture of *V*. As reflected in Figs. 2 and 3 many vacancies are bound to the dopant atoms and they are not associating with O_i to form A-centers. The quantitatively smaller binding of the Ge*V* pairs as compared to Pb*V* pairs implies that the former will be only stable at lower temperatures acting effectively as transient species. Conversely, the Pb*V* pair with their high binding energy will remain stable over a higher temperature range and thus affect more significantly not only the formation of *V*O pairs but also the conversion to VO_2 defects (refer to Figs. 2, 3).

From a reaction point of view in the case of the *V*O annealing the main contributing reactions are:

$$VO + O_i \rightarrow VO_2 \quad (5)$$

$$VO + Si_I \rightarrow O_i \quad (6)$$

In previous studies [38, 39], it was argued that due to the induced stains in the Si lattice by the larger isovalent dopants the balance between reactions (5) and (6) is shifted towards reaction (6), leading to the suppression of the VO_2 formation. In this framework the larger the isovalent dopant the larger the VO_2 suppression in agreement with Fig. 4. The calculations above show that the dopant strain energies and the strain in the lattice due to isovalent doping are small. This implies that they can play a significant role locally but not away from the vicinity of the dopant.

Another possibility that can be considered is the formation of Ge*V*O and Pb*V*O complexes via the following reactions:

$$Ge + VO \rightarrow GeVO \quad (7)$$

$$Pb + VO \rightarrow PbVO \quad (8)$$

Table 2 DFT derived binding energies (eV) of the Pb and Ge related defects in Si

Reaction	Binding energy
Ge + *V*O → Ge*V*O	−0.21[a]; −0.23[a]
Pb + *V*O → Pb*V*O	−1.17[a]; −1.26[a]
V + O → *V*O	−1.65[a]; −2.21[a]
Ge + *V* → Ge*V*	−0.25[a]; −0.26[a]; −0.27[b]
Pb + *V* → Pb*V*	−1.37[b]; −1.64[a]; −1.80[a]

Differences in energies are due to the different functionals employed

[a] Reference [38]

[b] Reference [37]

The DFT results (Ref. [40] and Table 2) indicate that both these reactions are energetically favourable and that a proportion of the migrating *V*O defects will be trapped by the isovalent atoms to form Ge*V*O and Pb*V*O defects. Both these defects are bound (again the isovalent atoms relax in the available volume offered by the *V* of the A-center) with Pb*V*O being more favourable by about 1 eV (refer to Table 2). Notably, experimental signals from these defects have not been identified so far in Ge-doped and Pb-doped Si. However, IR bands and DLTS peaks have been correlated [41] with various Ge*V*O structures in $Si_{1-x}Ge_x$. More specifically, two bands at 834.6 and 839.2 cm^{-1} were correlated [41, 42] with the Ge*V*O defect. Their presence of these defects is detected as a perturbation of the main IR band of *V*O at 830 cm^{-1} and Lorentzian analysis has demonstrated their characteristics. In Ge-doped Si these bands are expected to exist but at much lower concentration making their detection very difficult. In any case, they can be considered analogous to the Sn*V*O defects in Sn-doped Si [24].

Importantly, in high Sn-doped Si the Sn*V* and Sn*V*O defects have been correlated with the reduction of *V*O and its conversion to VO_2 [24]. We propose here a similar picture for Ge and Pb-doped Si. The difference between the two dopants is the higher binding energy for the Pb*V*O compared to the Ge*V*O defect, which implies that more *V*O defects will be associated with Pb as compared to Ge. This is turn will translate to a higher reduction of *V*O and its conversion to VO_2 for Pb-doped Si in agreement with the experimental results.

Let us consider the main reactions (5) and (6) that *V*O defect participates upon annealing and VO_2 defect forms. By summing up these two reactions we receive

$$2VO + Si_I \rightarrow VO_2 \quad (9)$$

The equilibrium constant K for this reaction is given by the expression:

$$K = \frac{[VO_2]}{[Si_I] \cdot [VO]^2} \quad (10)$$

and depends only on the temperature.

Now, for the case of Ge-doped or Pb-doped Si, Eq. (10) can be written as:

$$K_{Ge} = \frac{[VO_2]_{Ge}}{[Si_I]_{Ge} \cdot [VO]^2_{Ge}} \quad (11)$$

and

$$K_{Pb} = \frac{[VO_2]_{Pb}}{[Si_I]_{Pb} \cdot [VO]^2_{Pb}} \quad (12)$$

respectively.

Furthermore, the experimental evidence that the *V*O concentration is smaller in Pb-doped than in Ge-doped Si, that is $[VO]_{Pb} < [VO]_{Ge}$ can be expressed as follows:

$$[VO]_{Pb} = \lambda \cdot [VO]_{Ge} \quad (13)$$

where λ is dimensionless factor smaller than 1.

As the induced strains by the isovalent dopants were estimated to be small one can assume that the number of self-interstitials, $[Si_I]$ in reaction (9) has the same value for both cases of Ge and Pb, that is $[Si_I]_{Pb} \sim [Si_I]_{Ge}$. From Eqs. (12) and (13) we have:

$$K_{Pb} = \frac{[VO_2]_{Pb}}{[Si_I] \cdot \lambda^2 [VO]^2_{Ge}} \quad (14)$$

Now, due to the immutability of K ($K_{Pb} = K_{Ge}$) and via Eqs. (11) and (14) we have:

$$\frac{[VO_2]_{Ge}}{[Si_I] \cdot [VO]^2_{Ge}} = \frac{[VO_2]_{Pb}}{[Si_I] \cdot \lambda^2 [VO]^2_{Ge}}$$

from which we get to the relation

$$[VO_2]_{Pb} = \lambda^2 [VO_2]_{Ge} \quad (15)$$

Combining relations (13) and (15) we finally have:

$$\frac{[VO_2]_{Pb}}{[VO]_{Pb}} = \lambda \cdot \frac{[VO_2]_{Ge}}{[VO]_{Ge}} \quad (16)$$

Since $\lambda < 1$, the later relation confirms that a_{VO2}/a_{VO} is smaller in Pb than in Ge-doped Si. In other words the conversion ratio a_{VO2}/a_{VO} decreases with the increase of the dopant covalent radius, in agreement with our experimental findings (Fig. 4).

DFT calculations provide important information considering the association of Pb and Ge with carbon interstitials (C_i) and carbon substitutional (C_s) atoms. Previous DFT studies by Sgourou et al. [37] calculated that Pb is bound to both C_i and C_s forming PbC_i and PbC_s defects with binding energies −0.31 and −0.33 eV respectively (refer to Table 2). Conversely, Ge forms only GeC_i defects with binding energy −0.46 eV but not GeC_s defects [37]. These results favor the formation of Pb–C related defects rather than Ge–C defects. Therefore, the suppression of the C_iC_s and C_iO_i defects in Pb-doped Si will be more significant as compared to Ge-doped Si (consistently with Figs. 2, 3). Ge and Pb in the Si lattice may act as "scattering" centers for the diffusing C_i (refer to the case of $Si_{1-x}Ge_x$, Ref. [43]) leading to a retarded diffusion of the C_i and consequently to a suppression of the formation of the C_iO_i and the C_iC_s defects.

It can be observed from Fig. 4 that the ratio a_{CsO2i}/a_{CiOi} increases with the increase of the covalent radius. The C_sO_{2i} complex forms [44] upon the reaction $VO + C_iO_i \rightarrow C_sO_{2i}$ occurring at about 300 °C when both VO and C_iO_i defects become unstable and a small percentage of them associate to produce the C_sO_{2i} defect. As mentioned above Ge and Pb dopants react with C to form GeC_s, PbC_s and PbC_i defects. At temperatures of ~300 °C these defects may dissociate liberating C_s and C_i atoms. The latter are very mobile and are captured by oxygen atoms to form transient C_iO_i pairs, which react with VO defects to form additional C_sO_{2i} complexes. For the case of Pb doping the available at these temperatures carbon atoms ready to participate in the above processes are expected to be more numerous than in the case of Ge doping, leading to a larger number of C_sO_{2i} defects and finally enhancing the a_{CsO2i}/a_{CiOi} ratio. The opposite behavior exhibited between the conversion ratios a_{VO2}/a_{VO} and a_{CsO2i}/a_{CiOi} as a function of covalent radius may be related to the nature of the relevant defects. In particular the VO and VO_2 are vacancy-related, whereas the carbon-related defects C_iO_i to C_sO_{2i} involve self-interstitials in their formation.

Furthermore the annealing of the C_iC_s defect which contributes to the 546 cm^{-1} was accompanied in the spectra of Ge-doped Si (Fig. 2b) by the emergence of a weak band at 1,020 cm^{-1}. The identity of the defect giving rise to this band is unknown. It may have the same origin with photoluminescence (PL) lines at 951, 953, 954 and 957 meV reported [45, 46] to grow in the PL spectra upon the destruction of the 969 meV G-line arising from the C_iC_s. Notably, only traces of the 1,020 cm^{-1} band appear in the spectra Pb-doped Si (Fig. 2c) and its evolution cannot be shown in the figure.

Kinetics will also influence the picture as the introduction of oversized impurities in the lattice will impact diffusion properties. With the low concentrations considered in the present study their impact on diffusion is expected not to be global but rather concentrated at a radius of a few atomic sites around the isovalent atom. Again the impact of Pb will be far more significant compared to Ge as its covalent radius is far greater. These issues have been examined in previous DFT studies which have calculated that the migration energy barriers of vacancy-mediated diffusing species greatly increase in the presence of oversized isovalent atoms in group IV semiconductors. For example the study of Tahini et al. [47] calculated that the migration energy barriers for vacancy-mediated phosphorous diffusion are increased significantly in the presence of oversized isovalent dopants such as hafnium. The systematic investigation from a theoretical viewpoint of the impact of Pb on the energetics of A-center, C_iO_i and C_iC_s diffusion in Si may further clarify their formation and conversion.

The discussion above was focused on the engineering of oxygen-related (VO, VO_2) and C-related (C_iO_i, C_iC_s) radiation-induced defects in Si by Ge and Pb isovalent dopants. The results can be succinctly highlighted as follows:

(i) The suppression of the production of the *V*O and VO_2 defects was found to be related to the strains introduced in the lattice by the presence of larger Ge and Pb dopants. Although the strain fields were estimated to be weak, the calculated strain energies by the dopants indicate the capture of the vacancies by them (refer to Ge*V* and Pb*V* pairs) which finally reduce the *V*O and VO_2 production especially in Pb-doped Si. The role of Ge and Pb dopants due to the strain fields in their periphery, as annihilation centers for the vacancies and self interstitials, is another factor that should also be considered for the observed reductions. From a DFT perspective the formation of the Ge*V* and Pb*V* defects is confirmed, with the association of the Pb*V* being stronger consistently with the present calculations.

(ii) The reduction in the production of the *V*O and the VO_2 defects between Ge and Pb-doped Si does not necessarily imply a reduction in the corresponding conversion ratio a_{VO2}/a_{VO} of the *V*O to the VO_2 defect with the incease of the covalent radius. We have considered that the weak strain fields due to the presence of the Ge and Pb dopants in the Si lattice may not affect strongly the balance of the reactions (5) and (6), mainly responsible for the formation of the VO_2 defect upon the *V*O annealing. Subsequently, we have shown by thermodynamic arguments that the substantial reduction of the produced *V*O defects in the case of Pb as compared with that of Ge, for the reasons cited in (i), leads to a profound decrease of the conversion ratio a_{VO2}/a_{VO} for the Pb-doped Si.

(iii) The suppressed production of the C_iO_i and C_iC_s defects was attributed to the ability of the oversized Ge and Pb impurities to retard the migration of the C_i forward to the C_s and O_i impurities leading finally to a reduction in the formation of the C_iC_s and the C_iO_i pairs. Additionally, DFT calculations show the tendency of carbon to associate with Ge and Pb isovalent dopants and this can be a further reason for the reduction of the C_iO_i and C_iC_s defects.

(iv) Although most of the C_iO_i defects anneal out by dissociation at $\sim$300 °C, a small fraction of them converts to the C_sO_{2i} complex. Ge and Pb seems to enhance this ratio and the phenomenon was tentatively attributed to the release of carbon atoms from isovalent dopants-carbon pairs at these temperatures leading to the formation of transient C_iO_i pairs which in turn convert to C_sO_{2i} complexes.

5 Conclusions

Using FTIR spectroscopy it was determined that the production of *V*O, C_iO_i and C_iC_s defects in electron irradiated Si is reduced by the presence of isovalent dopants and in particular in the case of Pb. Upon annealing the conversion to secondary defects (*V*O to VO_2 and C_iO_i to C_sO_{2i}) is also affected by the isovalent dopants. Notably, the conversion ratios are reduced more for Pb doping. The calculation of the dopant strain in the lattice due to isovalent doping revealed that is limited for the dopant concentrations considered. However, the strain energies are substantially higher in the case of Pb-doping and can justify indirectly the presence of Pb*V* defects. Using recent DFT results we propose that the Pb and Ge doping influences the production and conversion of the *V*O, C_iO_i and C_iC_s defects via the formation of Pb*V*, Pb*V*O, PbC_i, PbC_s, Ge*V*, Ge*V*O and GeC_i defects. The present work indicates the ability of engineering O- and C-related radiation defects in Si.

References

1. S.G. Cloutier, P.A. Kossyrev, J. Xu, Nat. Mater. **4**, 877 (2005)
2. A. Chroneos, C.A. Londos, J. Appl. Phys. **107**, 093518 (2010)
3. K. Murata, Y. Yasutake, K. Nittoh, S. Fukatsu, K. Miki, AIP Adv. **1**, 032125 (2011)
4. D.D. Berhanuddin, M.A. Lourenço, R.M. Gwilliam, K.P. Homewood, Adv. Funct. Mater. **22**, 2709 (2012)
5. C. Gao, X. Ma, J. Zhao, D. Yang, J. Appl. Phys. **113**, 093511 (2013)
6. C.A. Londos, E.N. Sgourou, A. Chroneos, J. Mater. Sci. Mater. Electron. **24**, 1696 (2013)
7. A. Chroneos, J. Appl. Phys. **105**, 056101 (2009)
8. A. Chroneos, C.A. Londos, E.N. Sgourou, J. Appl. Phys. **110**, 093507 (2011)
9. H. Tahini, A. Chroneos, R.W. Grimes, U. Schwingenschlogl, A. Dimoulas, J. Phys. Condens. Matter **24**, 195802 (2012)
10. P. Chen, X. Yu, X. Liu, X. Chen, Y. Wu, D. Yang, Appl. Phys. Lett. **102**, 082107 (2013)
11. J.W. Corbett, G.D. Watkins, R.S. McDonald, Phys. Rev. **135**, 1381 (1964)
12. C.A. Londos, L.G. Fytros, G.J. Georgiou, Defects Diffus. Forum **171–172**, 1 (1999)
13. G. Davies, R.C. Newman, in *Handbook of Semiconductors*, vol. 3, ed. by S. Mahajan (Elsevier, Amsterdam, 1994), pp. 1557–1635
14. E.V. Lavrov, L. Hoffmann, B.B. Nielsen, Phys. Rev. B **60**, 8081 (1999)
15. C.A. Londos, M.S. Potsidi, E. Stakakis, Phys. B **340–342**, 551 (2003)
16. L.I. Murin, V.P. Markevich, J.L. Lindstrom, M. Kleverman, J. Hermansson, T. Halberg, B.G. Svensson, Solid State Phenom. **82–84**, 57 (2002)
17. C.-L. Liu, W. Windl, L. Borucki, S. Lu, X.-Y. Liu, Appl. Phys. Lett. **80**, 52 (2002)
18. F. Zirkelbach, B. Stritzker, K. Nordlund, J.K.N. Lindner, W.G. Schmidt, E. Rauls, Phys. Rev. B **82**, 064126 (2011)

19. H. Wang, A. Chroneos, C.A. Londos, E.N. Sgourou, U. Schwingenschlögl, Sci. Rep. **4**, 4909 (2014)
20. S.D. Brotherton, P. Bradley, J. Appl. Phys. **53**, 5720 (1982)
21. A. Khan, M. Yamaguchi, Y. Ohshita, N. Dharmarasu, K. Araki, T. Abe, H. Itoh, T. Ohshima, M. Imaizumi, S. Matsuda, J. Appl. Phys. **90**, 1170 (2001)
22. C.A. Londos, Phys. Stat. Solidi (a) **113**, 503 (1989)
23. H. Höhler, N. Atodiresei, K. Schroeder, R. Zeller, P.H. Dederichs, Phys. Rev. B **71**, 035212 (2005)
24. A. Chroneos, C.A. Londos, E.N. Sgourou, P. Pochet, Appl. Phys. Lett. **99**, 241901 (2011)
25. H. Wang, A. Chroneos, C.A. Londos, E.N. Sgourou, U. Schwingenschlögl, Appl. Phys. Lett. **103**, 052101 (2013)
26. M.L. David, E. Simoen, C. Claeys, V. Neimash, M. Kras'ko, A. Kraitchinskii, V. Voytovych, A. Kabaldin, J.F. Barbot, Solid State Phenom. **108–109**, 373 (2005)
27. V.B. Neimash, V.V. Voitovych, A.M. Kraitchinskii, L.I. Shpinar, M.M. Kras'ko, V.M. Popov, A.P. Pokanevych, M.I. Gorodys'kyi, Y.V. Pavlovs'kyi, V.M. Tsmots, O.M. Kabaldin, Ukr. J. Phys. **50**, 492 (2005)
28. X. Yu, P. Wang, P. Chen, X. Li, D. Yang, Appl. Phys. Lett. **97**, 051903 (2010)
29. M. Aviranandhan, R. Gotoh, T. Watahiki, K. Fujiwara, Y. Hayakawa, S. Uda, M. Konagai, J. Appl. Phys. **111**, 043707 (2012)
30. C.A. Londos, E.N. Sgourou, A. Chroneos, V.V. Emtsev, Semicond. Sci. Technol. **26**, 105024 (2011)
31. C.A. Londos, E.N. Sgourou, D. Timerkaeva, A. Chroneos, P. Pochet, V.V. Emtsev, J. Appl. Phys. **114**, 113504 (2013)
32. E.N. Sgourou, A. Andrianakis, C.A. Londos, A. Chroneos, J. Appl. Phys. **113**, 113507 (2013)
33. E.N. Sgourou, C.A. Londos, A. Chroneos, J. Appl. Phys. **116**, 133502 (2014)
34. K. Weiser, J. Phys. Chem. Solids **7**, 118 (1958)
35. P.A. Varotsos, K.D. Alexopoulos, Thermodynamics of point defects and their relation with bulk properties. Defects Solids **14**, 328 (1986)
36. S.N. Vaidya, G.C. Kennedy, J. Phys. Chem. Solids **33**, 1377 (1972)
37. E.N. Sgourou, D. Timerkaeva, C.A. Londos, D. Aliprantis, A. Chroneos, D. Caliste, P. Pochet, J. Appl. Phys. **113**, 113506 (2013)
38. C.A. Londos, A. Andrianakis, E.N. Sgourou, V.V. Emtsev, H. Ohyama, J. Appl. Phys. **109**, 033508 (2011)
39. C.A. Londos, D. Aliprantis, E.N. Sgourou, A. Chroneos, P. Pochet, J. Appl. Phys. **111**, 123508 (2012)
40. H. Wang, A. Chroneos, C.A. Londos, E.N. Sgourou, U. Schwingenschlögl, Phys. Chem. Chem. Phys. **16**, 8487 (2014)
41. V.P. Markevich, A.R. Peaker, J. Coutinho, R. Jones, V.J.B. Torres, S. Oberg, P.R. Briddon, L.I. Murin, L. Dobaczewski, N.V. Abrosimov, Phys. Rev. B **69**, 125218 (2004)
42. YuV Pomozov, M.G. Sosnin, L.I. Khirunenko, V.I. Yashnik, N.V. Abrosimov, M. Hohne, Semiconductors **34**, 989 (2000)
43. A.N. Larsen, A.B. Hansen, D. Reitze, J.J. Coubel, J. Fage-Pedersen, A. Mesli, Phys. Rev. B **64**, 233202 (2001)
44. N. Inoue, H. Ohyama, Y. Goto, T. Sugiyama, Phys. B **401–402**, 477 (2007)
45. G. Davies, Mater. Sci. Forum **38–41**, 151 (1989)
46. G. Davies, E.C. Lightowlers, M.C. doCarmo, J.G. Wilkes, G.R. Wolstenholme, Solid State Commun. **50**, 1057 (1984)
47. H.A. Tahini, A. Chroneos, R.W. Grimes, U. Schwingenschlögl, H. Bracht, Phys. Chem. Chem. Phys. **15**, 367 (2013)